Signaling preferences of substituted pyrrole coupled six-membered spirocyclic rhodamine probes towards Hg^{2+} ion detection

Biswonath Biswal, Debajani Mallick, Bamaprasad Bag*

Colloids and Materials Chemistry Department, Academy of Scientific and Innovative Research, CSIR-Institute of Minerals and Materials Technology, P.O.: R.R.L., Bhubaneswar-751 013, Odisha, India.
Fax: (+) 91 674 258 1637; Tel: (+ 91) 674 237 9254, Email: bpbag@immt.res.in

Electronic Supplementary Information

Experimental

All the reagent grade chemicals were used without purification unless otherwise specified. 2,4-dimethyl pyrrole carboxaldehyde, rhodamine B base and the metal-perchlorate salts were obtained from Sigma–Aldrich (India) and used as received. Anhydrous sodium sulphate, sodium borohydride, silica gel for column chromatography, acids and the solvents were received from Spectrochem Pvt Ltd (India). All the solvents were freshly distilled prior to use for absorption and fluorescence measurements.

Fluorescence quantum yields were determined by comparing the corrected spectrum with that of rhodamine G ($\phi_F = 0.95$) in EtOH by taking area under total emission using following eqn.,

$$\phi_S = \phi_R \left(\frac{F_S A_R}{F_R A_S}\right) \cdot \left(\frac{\eta_S}{\eta_R}\right) \qquad \text{..... ..... eqn. S1}$$

where ϕ_S and ϕ_R are radiative quantum yields, F_S and F_R are area under the fluorescence spectra, A_S and A_R are absorbances (at the excited wavelength) of respective samples and the reference respectively; η_S and η_R are the refractive indices of the solvent used for the sample and the reference. The quantum yield of Rhodamine G was measured using quinine sulfate in 1N H_2SO_4 as reference excited at (λ_{ex}) 350 nm. The standard quantum yield value thus obtained was used for the calculation of the quantum yield of the samples.

The graphical representations of synthesized compounds are given in Scheme S1 for quick reference.

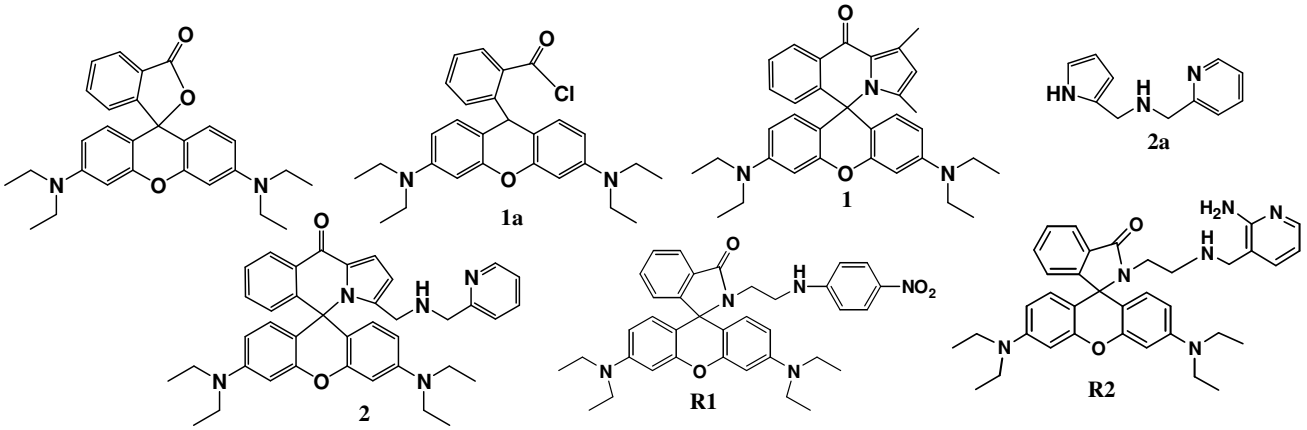

Scheme S1: Structure of the compounds

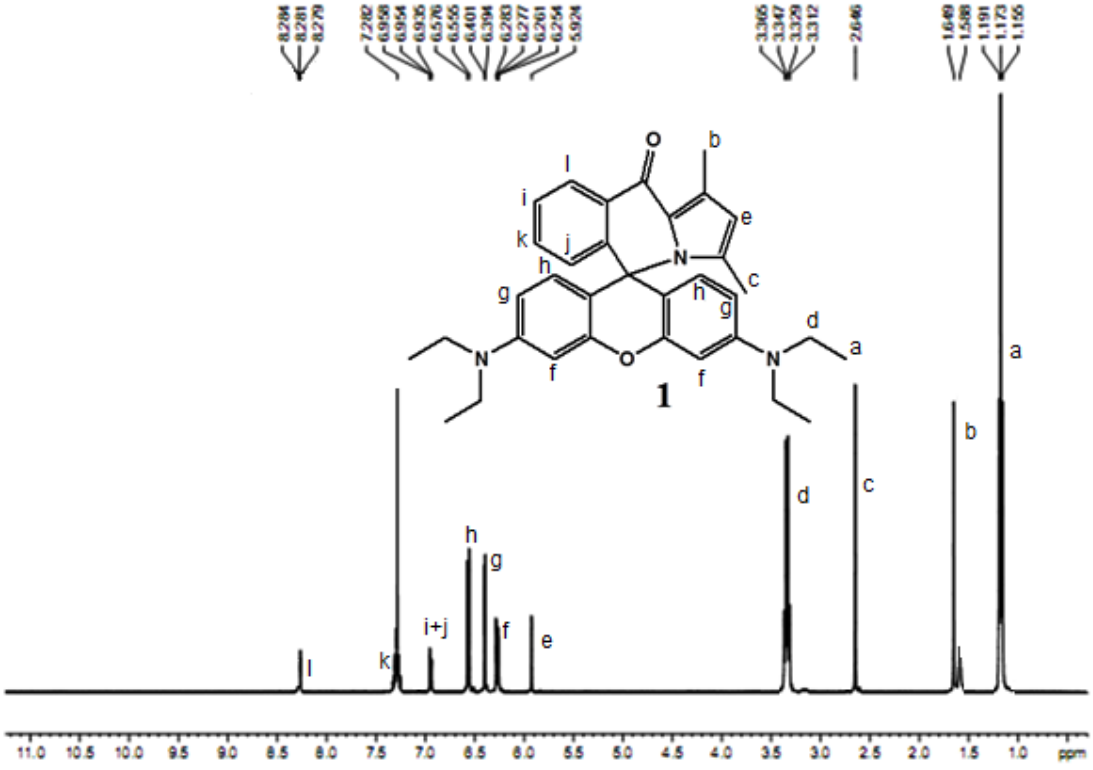

Fig. S1: ^{1}H-NMR spectrum of **1** in $CDCl_3$.

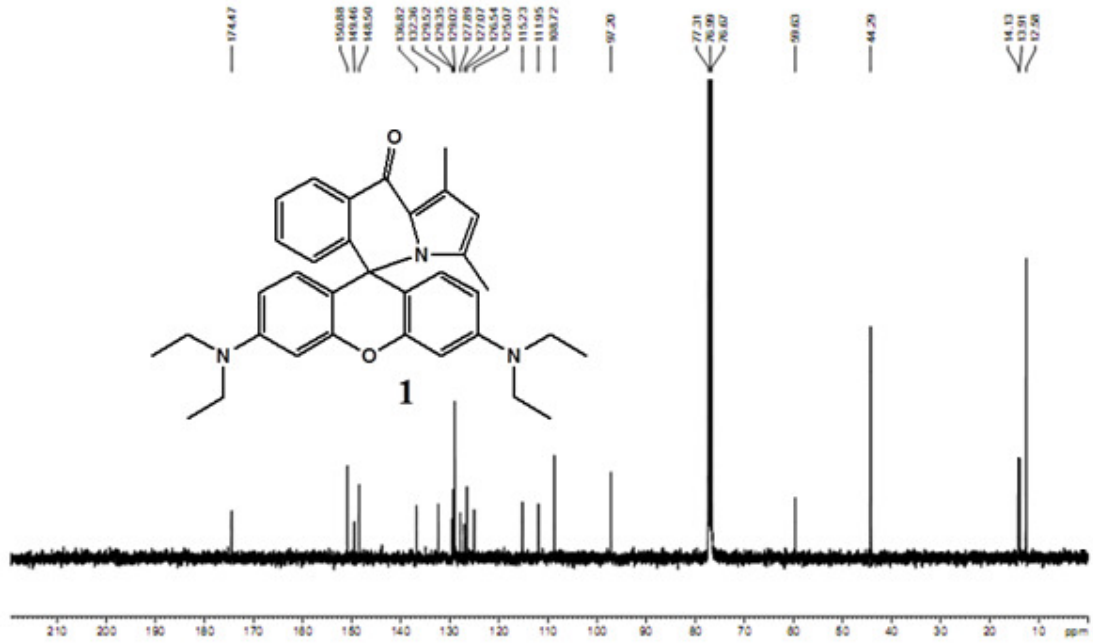

Fig. S2: ^{13}C-NMR spectrum of **1** in $CDCl_3$.

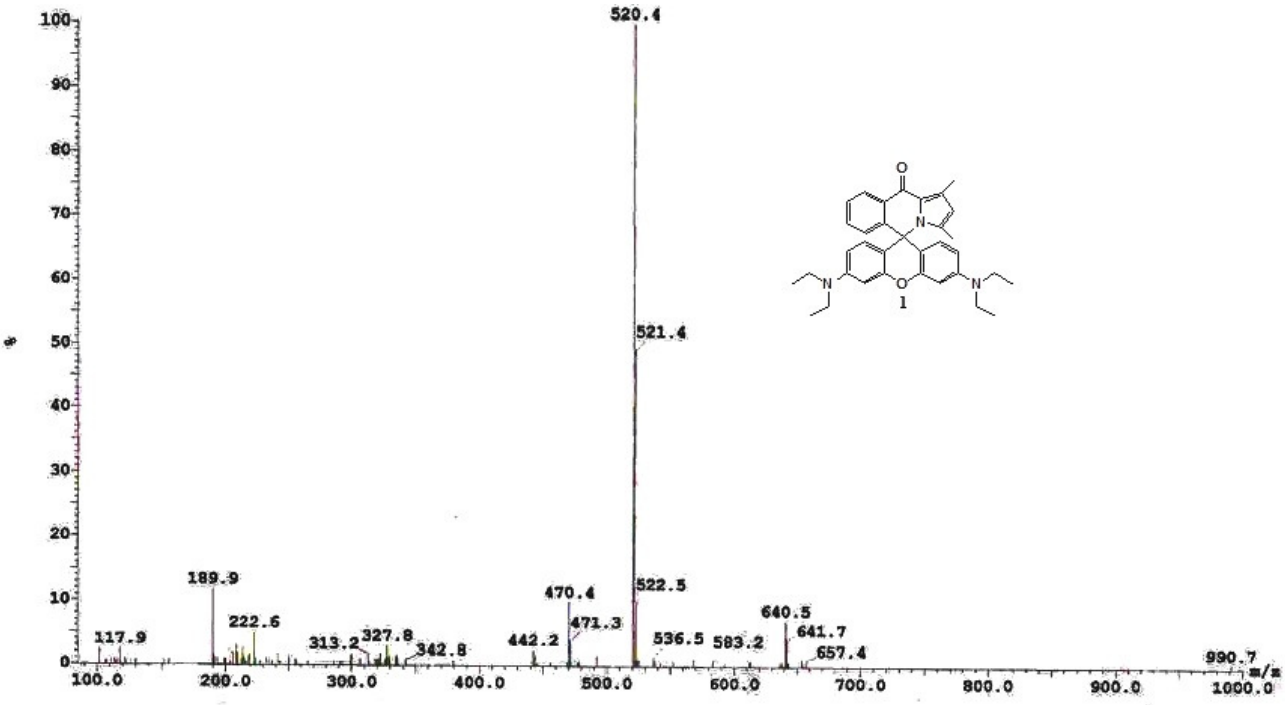

Fig. S3: ESI-MS spectrum of **1**

Fig. S4: ^{1}H-NMR spectrum of **2a** in $CDCl_3$.

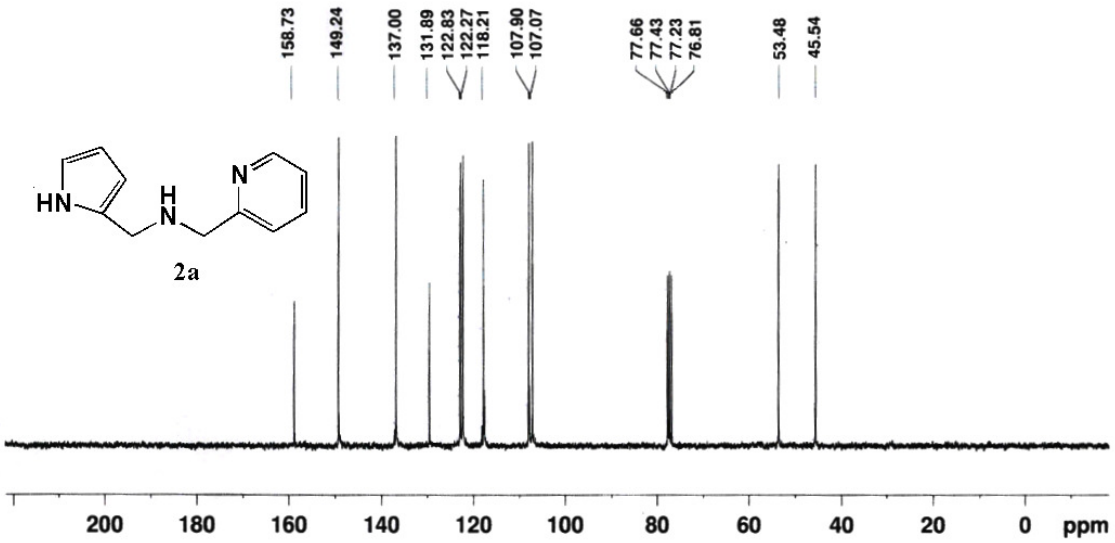

Fig. S5: ^{13}C-NMR spectrum of **2a** in $CDCl_3$.

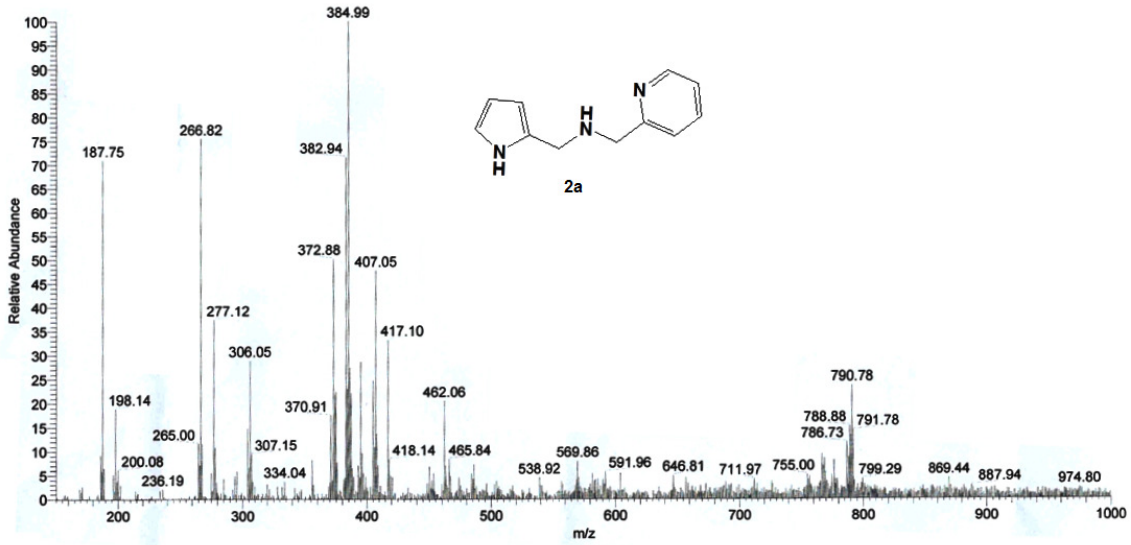

Fig. S6: ESI-MS spectrum of **2a**

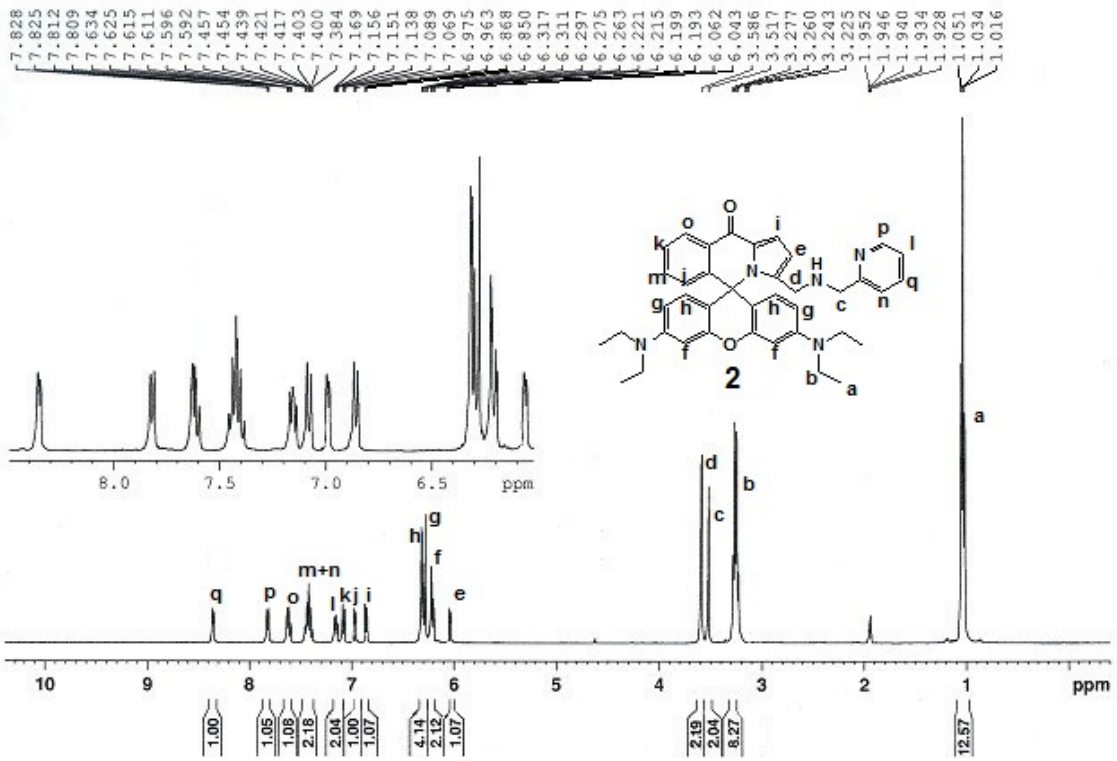

Fig. S7: ^{1}H-NMR spectrum of **2** in CD_3CN.

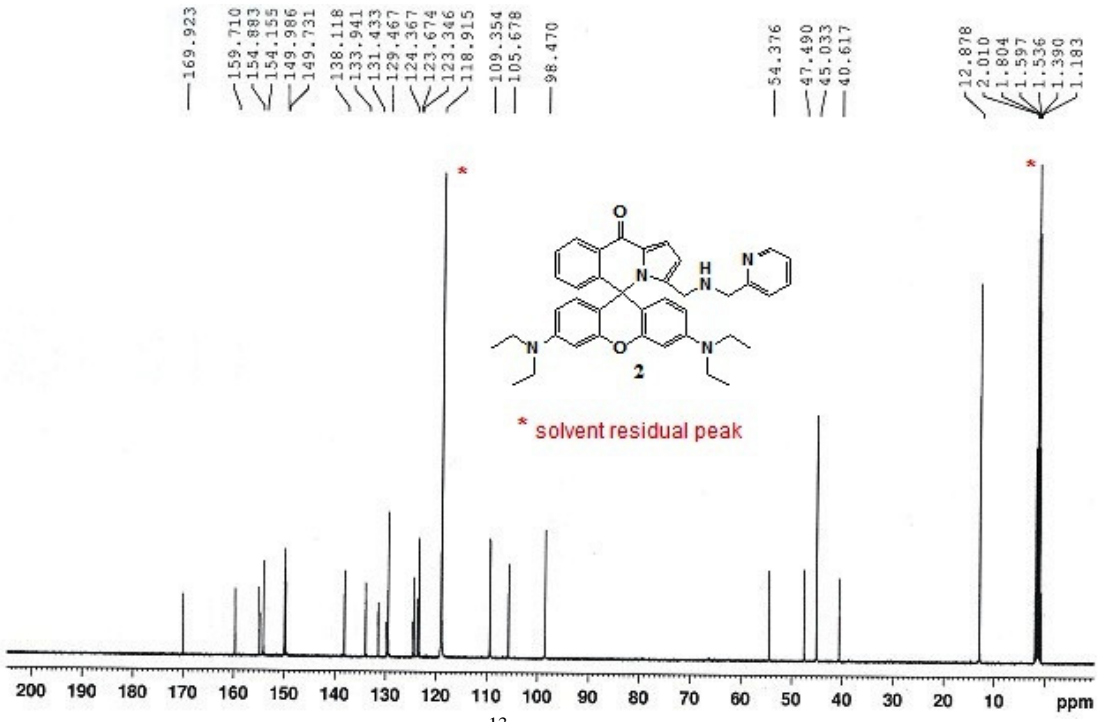

Fig. S8: ^{13}C-NMR spectrum of **2** in CD_3CN.

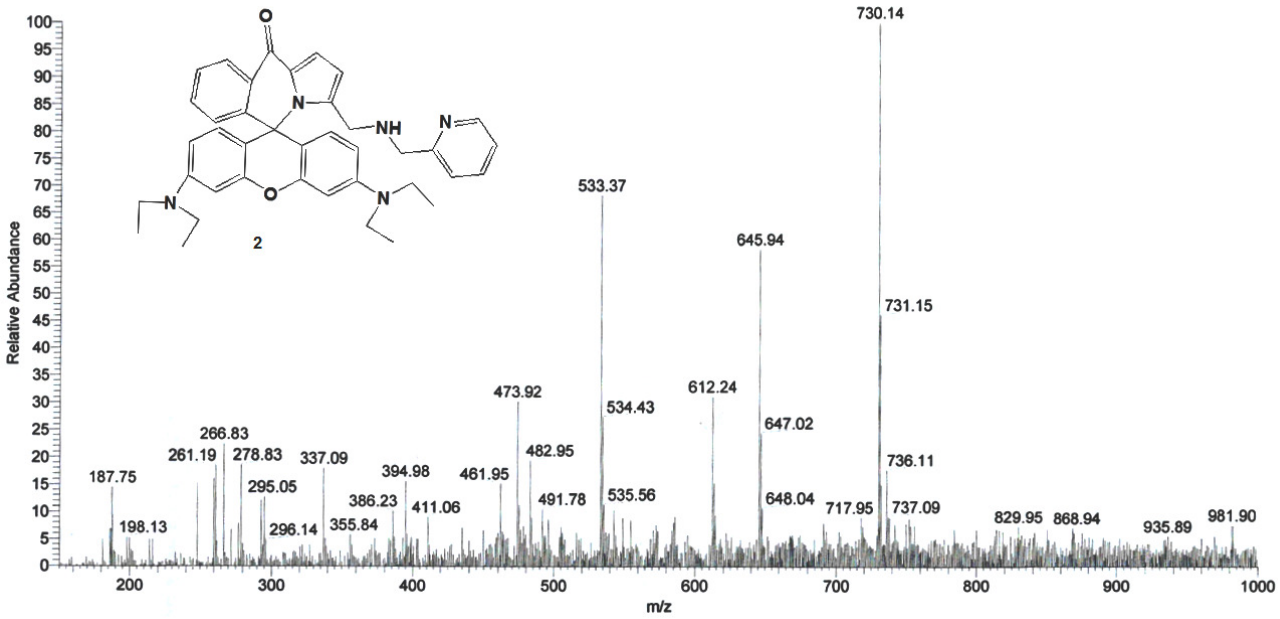

Fig. S9: ESI-MS spectrum of **2**

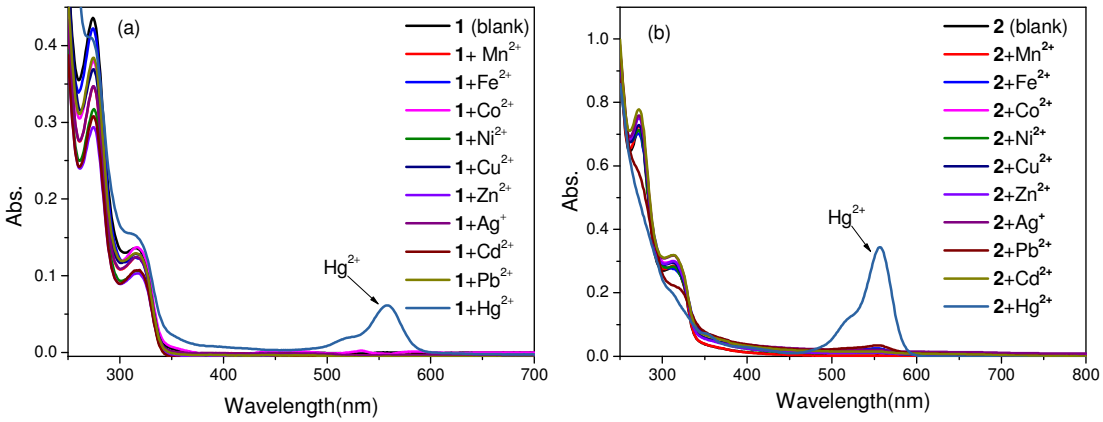

Fig. S10: Absorption spectra of (a) **1** and (b) **2** in presence of various metal ions. [**1** or **2**] = 10μM, MeCN-H_2O (1:1 v/v, pH 7.2).

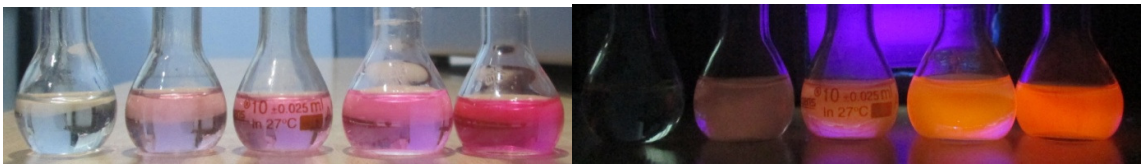

Fig. S11: Change in colour in the solution of **1**(2×10^{-5}M) in MeCN-H_2O (1:1 v/v, pH 7.2) upon addition of 0, 1, 2, 3 and 5 eq. of Hg^{2+} under (a) normal light and (b) upon irradiation at 450nm.

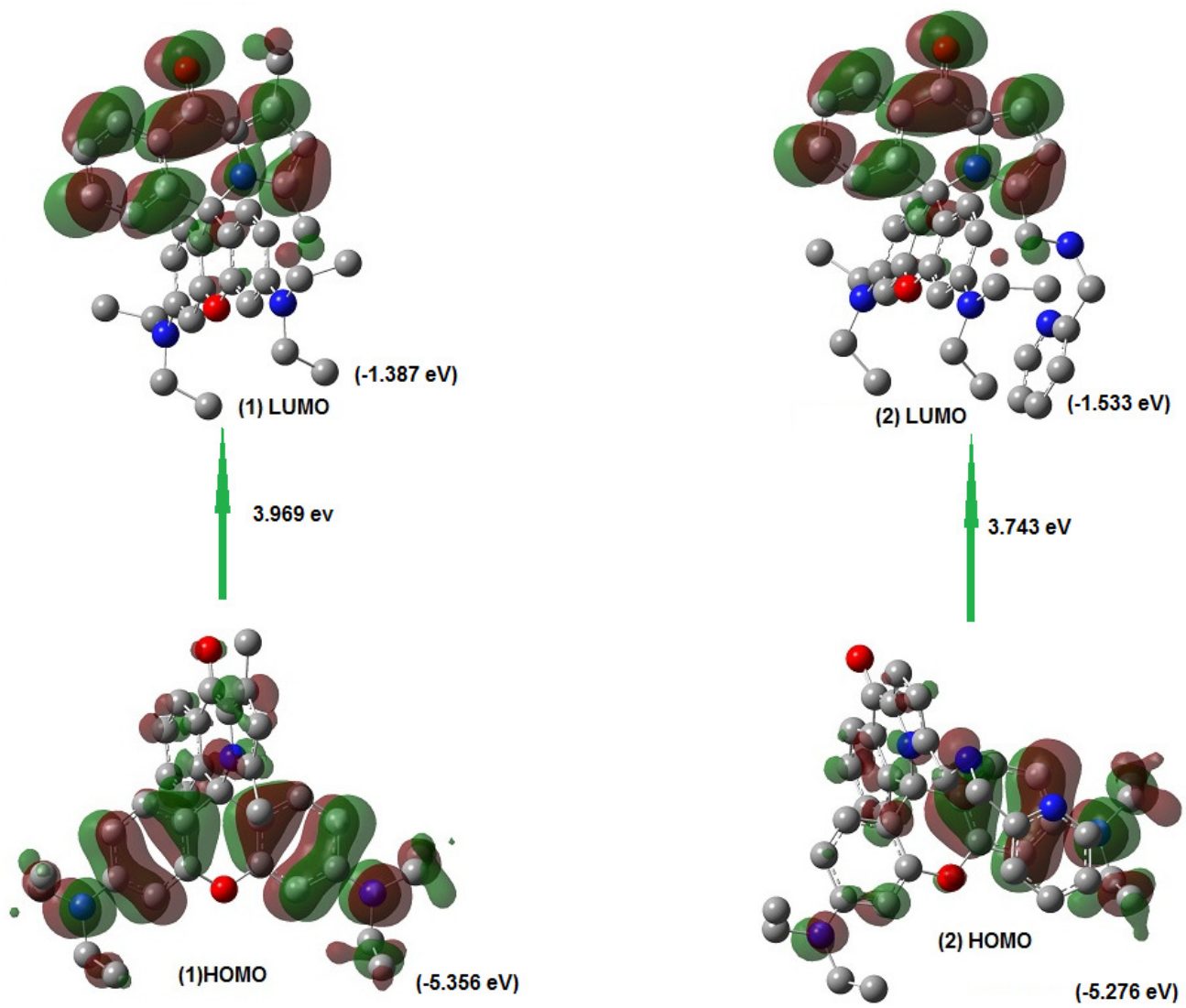

Fig. S12: Ground state HOMO and LUMO of **1**(left) and **2**(right) as elucidated from DFT calculations. The energies of frontier orbitals and corresponding distribution of π-electrons shows that the electron densities located over xanthene ring in HOMO while those over spiro-ring in LUMO. The HOMO-LUMO energy gap shows that these probes do not absorb in the visible region, rather exhibits absorption transitions at 312 nm (**1**) and 331 nm(**2**) respectively, which is complemented well to the experimental observations.

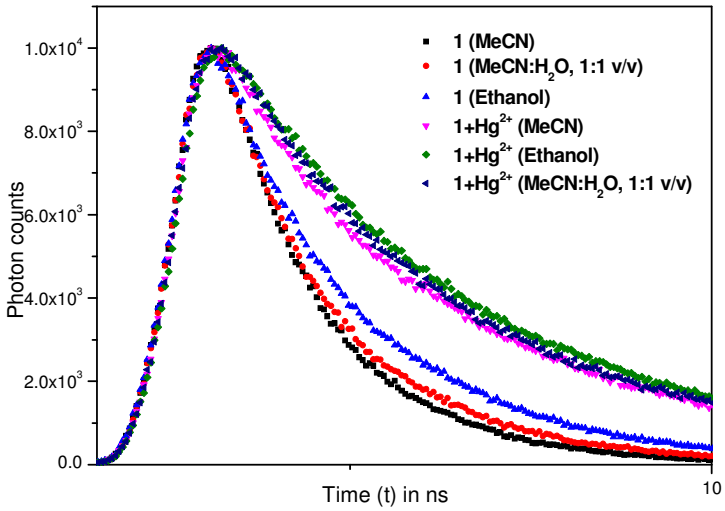

Fig S13: Time-resolved fluorescence exponentially fitted decay profile of **1** in absence and presence of Hg^{2+} ion in MeCN, MeCN-H_2O (1:1 v/v) and EtOH medium.

Table ST-1: Fit-results to the exponential decay curve obtained with time-correlated single photon counting technique with single exponential fit equation A+B exp (-t/τ)

Solvent	MeCN:H_2O (1:1 v/v)		MeCN		EtOH	
	1	**1**+Hg^{2+}	**1**	**1**+Hg^{2+}	**1**	**1**+Hg^{2+}
τ (av., ns)	1.572	5.682	1.918	6.084	1.465	4.070
A	8.819	16.306	7.532	16.212	9.446	15.806
B	6816.138	10191.604	7875.959	10820.598	9318.325	9312.714
σ (std. dev.)	44.2667	29.4258	54.6974	29.6571	69.8257	59.2583
χ^2	1.234	1.075	1.161	1.284	1.179	1.051

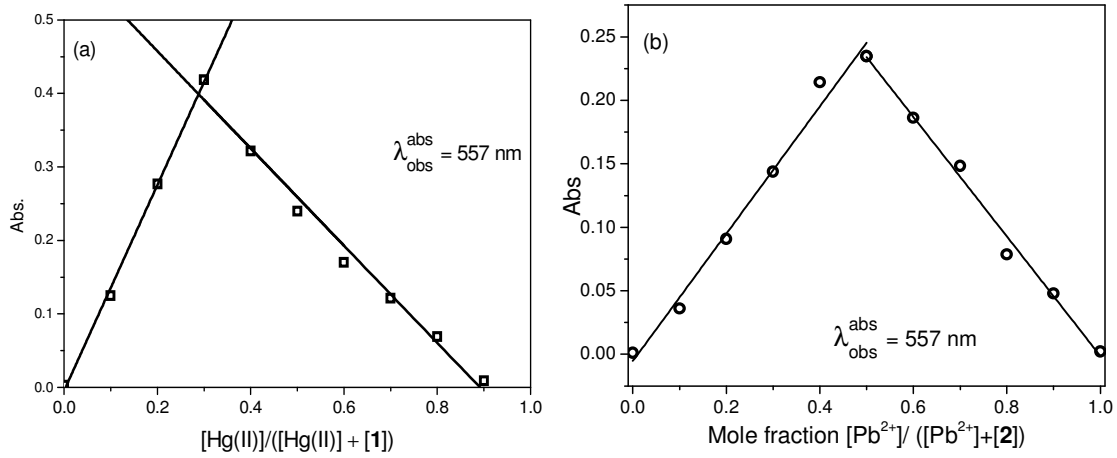

Fig. S14: Change in absorption as a function of mole fraction of added metal ion(Job's plot) for determination of complexation stoichiometry, (a) **1** with Hg^{2+} and (b) **2** with Pb^{2+} ion respectively.

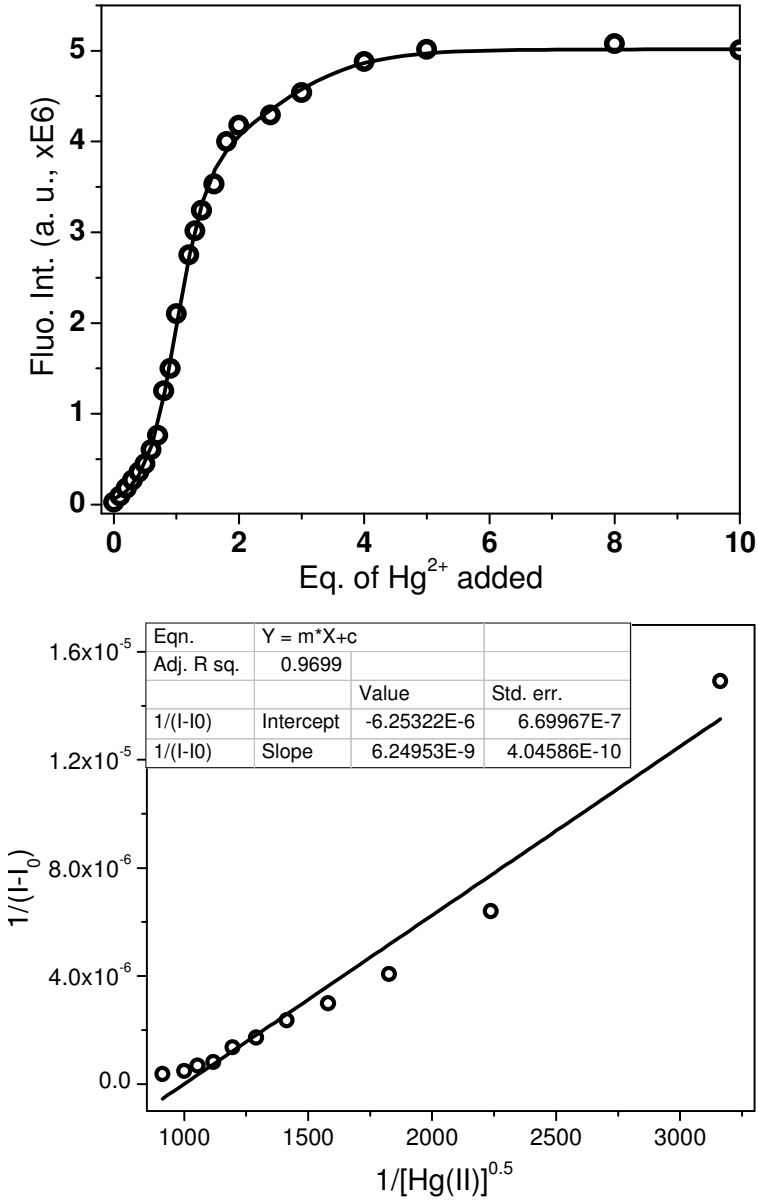

Fig. S15: (a) Plot of change in fluorescence intensity of **1** as a function of added [Hg(II)] ions in MeCN-H_2O (1:1 v/v). Experimental conditions: [**1**] = 5 × 10^{-7} M, λ_{ex} = 500 nm, RT, *ex.* and *em.* b. p. = 5nm; (b) Linear regression to the double reciprocal plot of fluorescence intensity change{$1/(I-I_0)$} against added metal ion ($1/[Hg^{2+}]^{0.5}$) for determination of complex stability constant for 2:1 (**1**:Hg^{2+}) complexation stoichiometry.

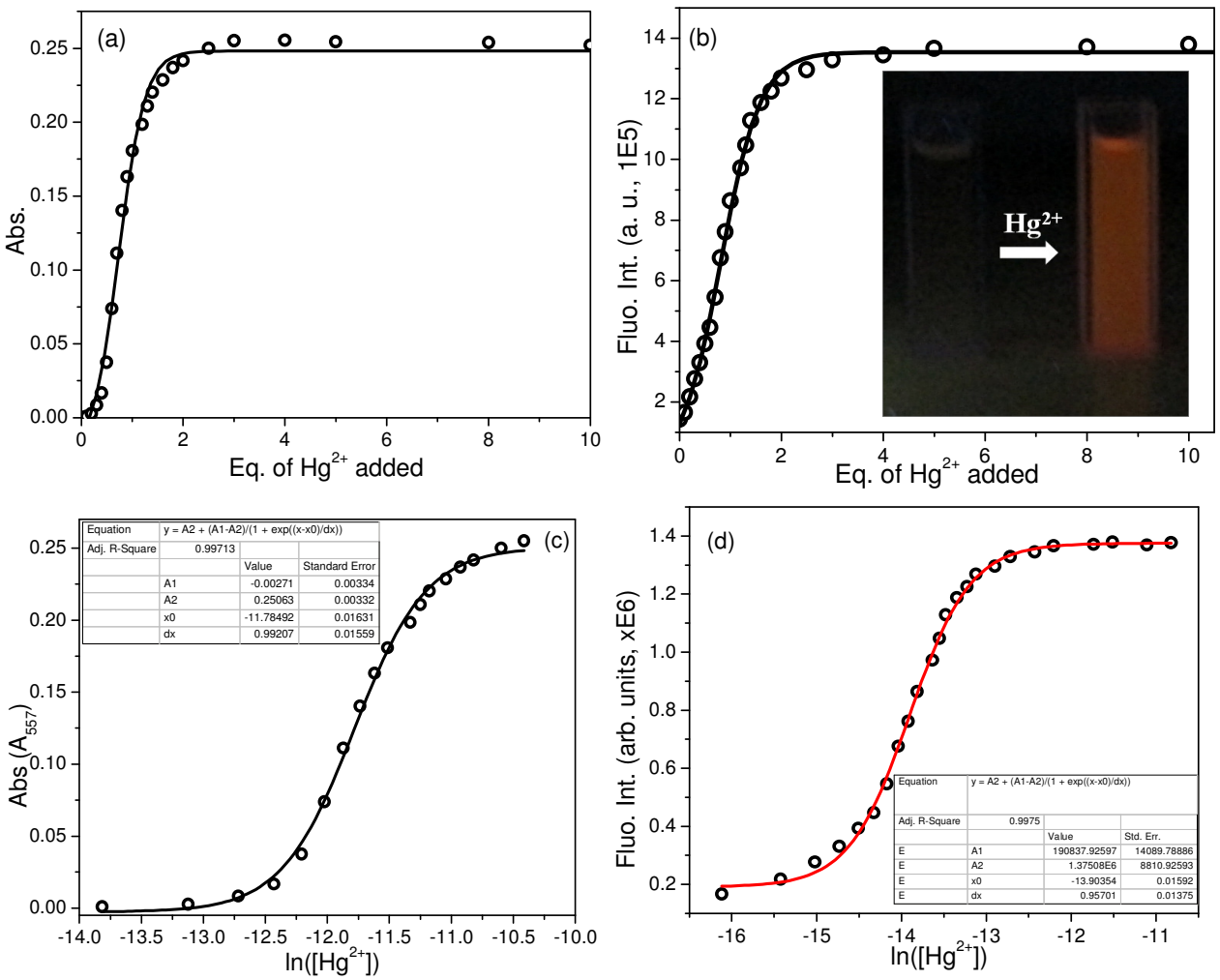

Fig. S16: (a) Plot of change in (a) absorption and (b) fluorescence intensity of **2** as a function of added [Hg^{2+}] ions in MeCN-H_2O (1:1 v/v). Inset(b): change in colour of the solution of **2** in presence of Hg^{2+} when irradiated with 450nm light. Non-linear regression to the plot of (c) absorption and (d) fluorescence intensity against added metal ion (ln[Hg^{2+}]). Experimental conditions: emission [**2**] = 5×10^{-7} M, λ_{ex} = 500 nm, RT, *ex.* and *em.* b. p. = 5nm.

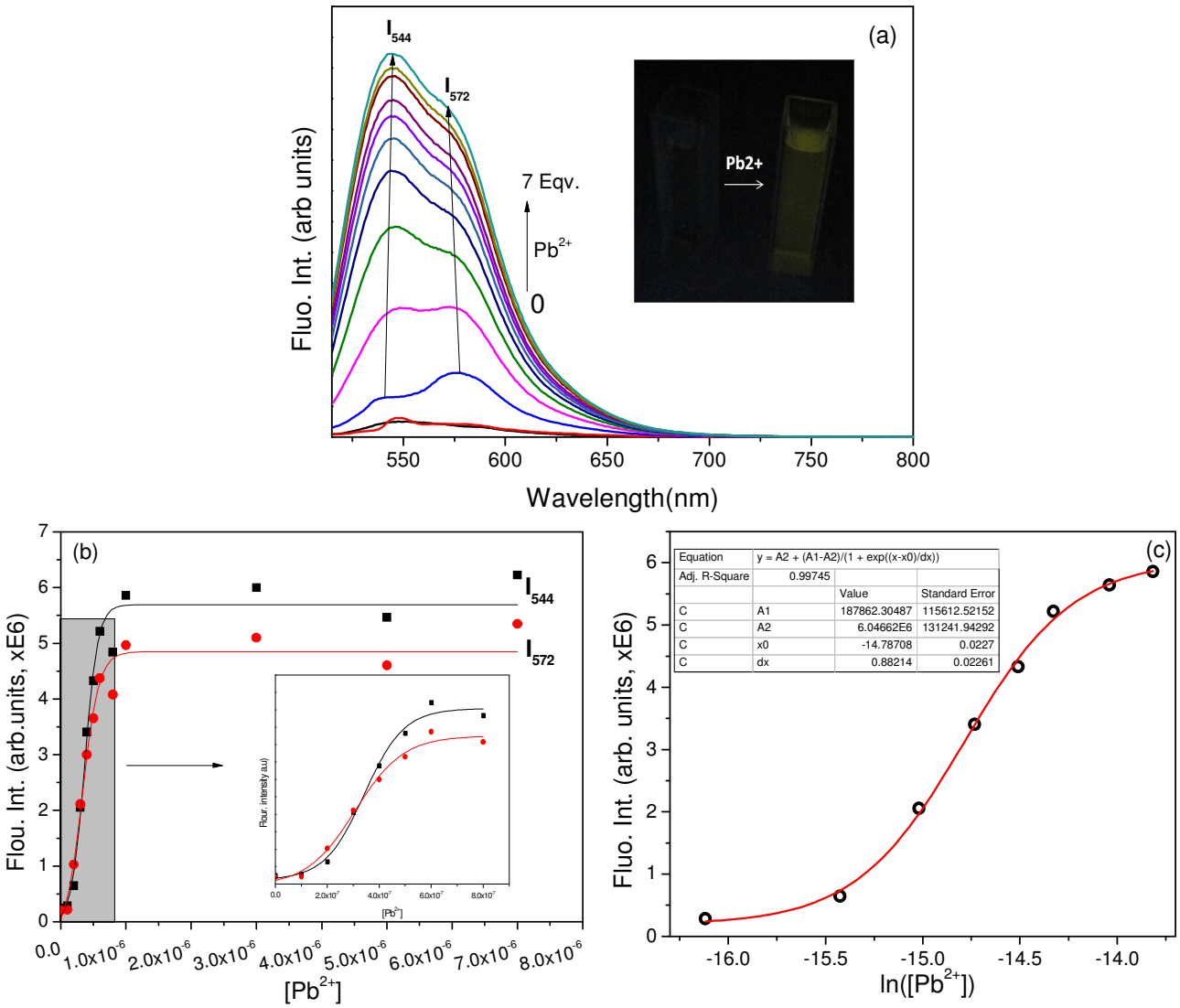

Fig. S17: (a) Fluorescence spectra of **2** as a function of equivalents of added Pb^{2+} ion and (b) its corresponding spectral profile at 644nm and 672nm respectively. (Inset, a) Change in colour of the solution of **2** in presence of Pb^{2+} when irradiated with 450 nm light. (c) Non-linear regression to the plot of corresponding fluorescence intensity against added metal ion ($ln[Pb^{2+}]$). Experimental conditions: emission [**2**] = 5×10^{-7} M, λ_{ex} = 500 nm, RT, *ex.* and *em.* b. p. = 5nm.

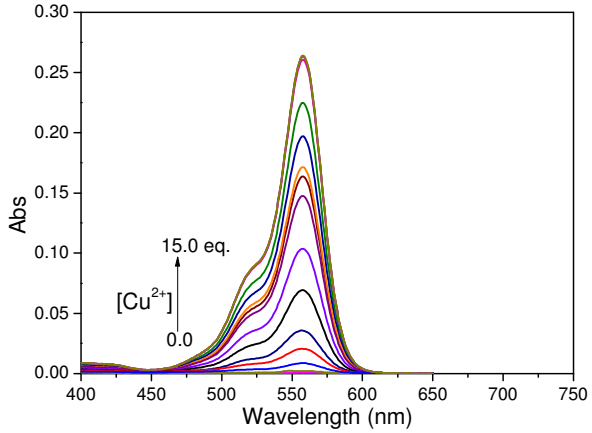

Fig. S18: Absorption spectra of **2** (1×10^{-4}M) in MeCN-H_2O (1:1 v/v, PBS, pH 7.2) as a function of equivalents of added Cu^{2+} ion.

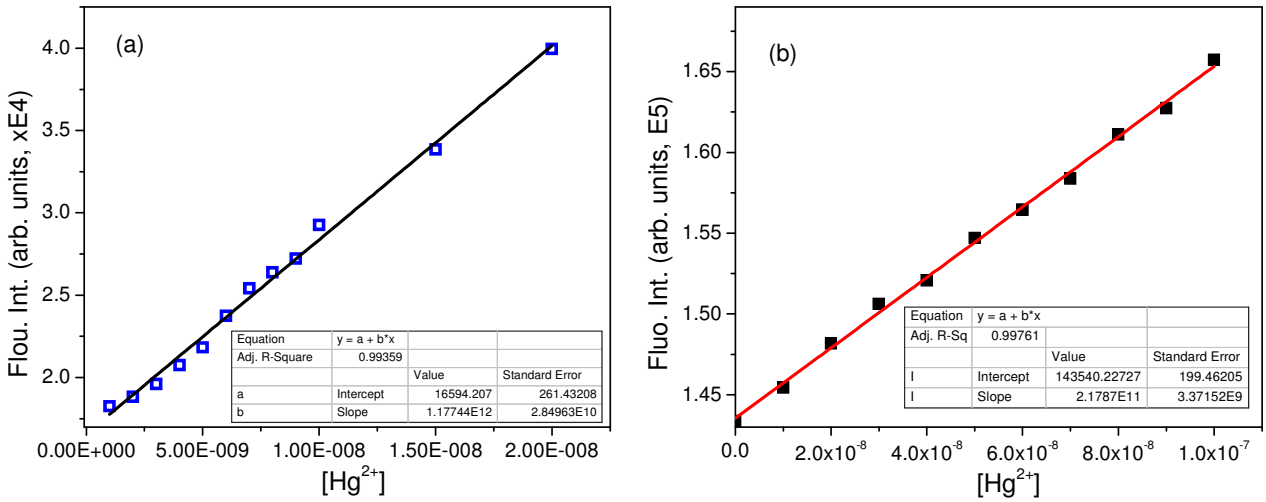

Fig. S19: Linear regression of fluorescence spectral intensities of (a) **1** and (b) **2** with added Hg^{2+} ion for determination of sensitivity of Hg^{2+} detection.

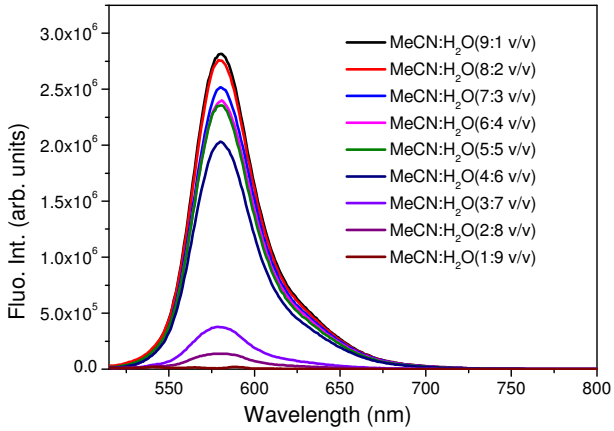

Fig. S20: Fluorescence spectra of **1** in presence of $Hg(ClO_4)_2$ (5 eq.) in varied proportion of binary solvent composition (MeCN:H_2O, v/v, PBS). [**1**] = 2μM, λ_{ex} = 500nm, RT, ex. and em. b p = 5nm.

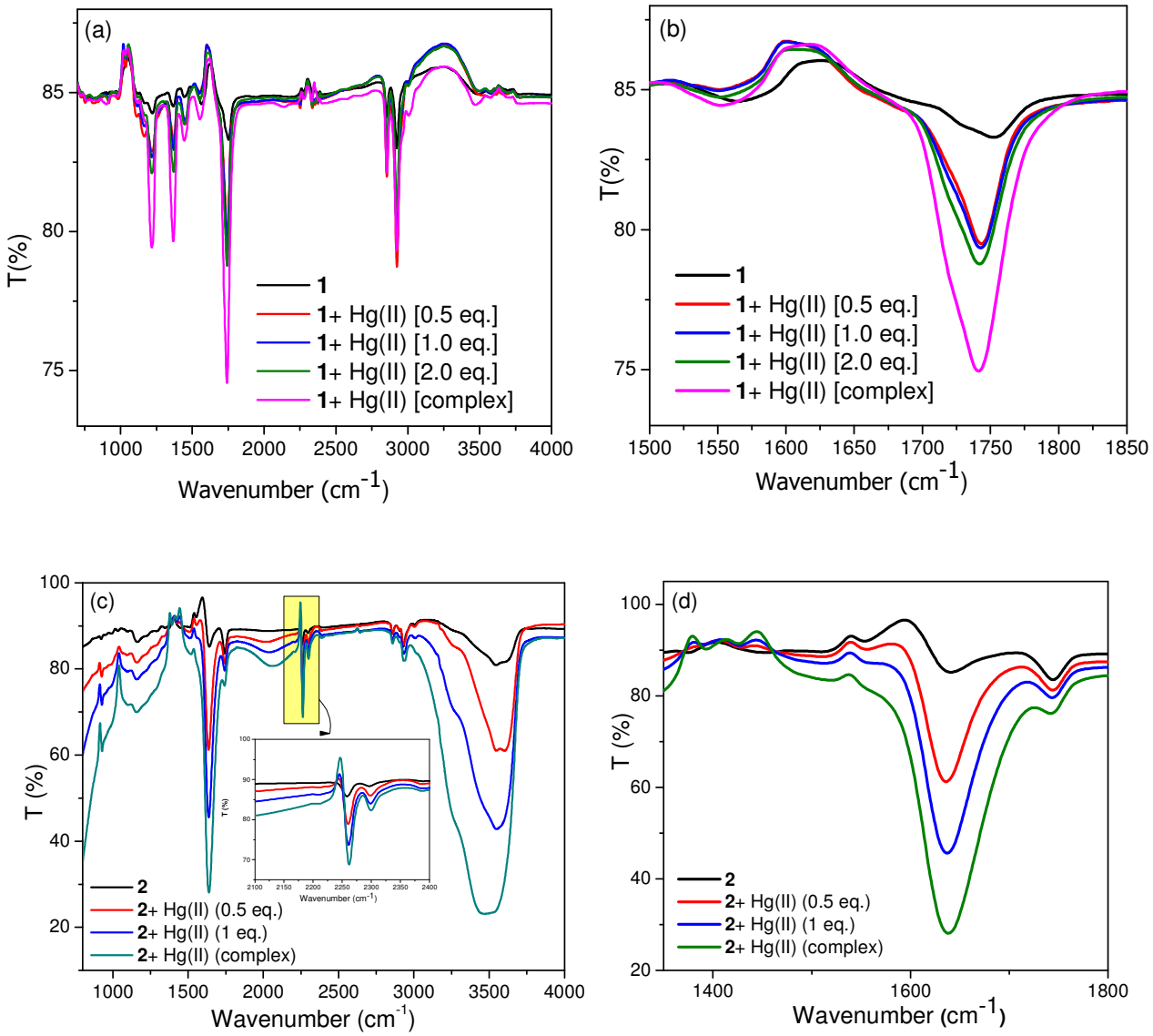

Fig. S21: FT-IR spectra of **1** (a and b) and **2** (c and d) alone and in presence of Hg^{2+} ion in solution.

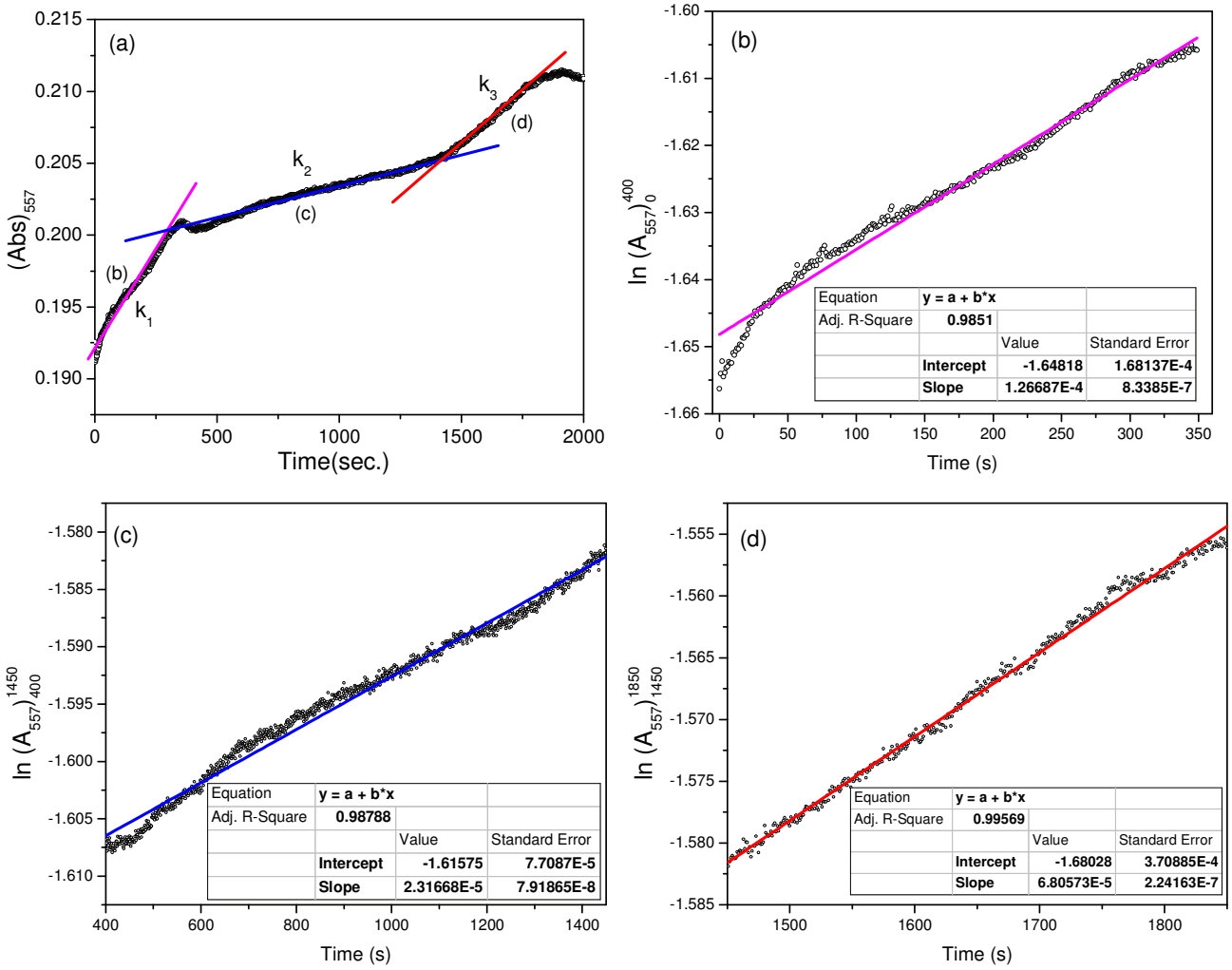

Fig. S22: (a) Change in absorption (A_{557}) in **1**(10 μM) when added Hg^{2+} ion as a function of time (s) in MeCN-H_2O (1:1 v/v, PBS, pH 7.2). Figures (b), (c) and (d) represents linear regression plots of ln(A_{557}) against time for determination of rate constant (k) of first-order kinetics at the desired time interval.

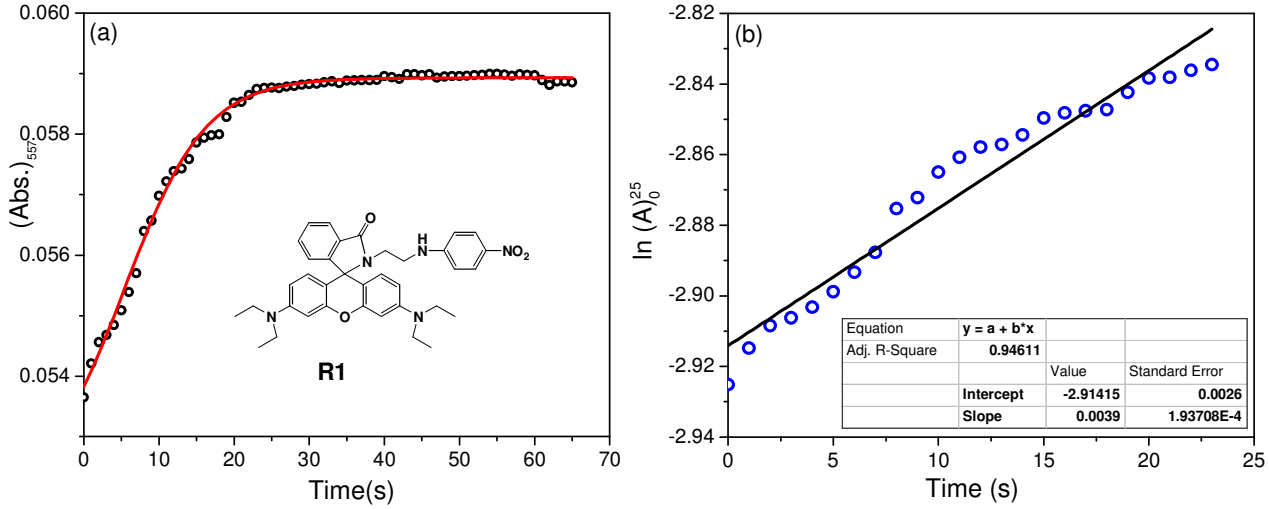

Fig. S23: (a) Change in absorption (A_{557}) in **a five membered spiro-ring based probe R1** (4 μM) when Hg^{2+} ion added (1:1 stoichiometry) as a function of time (s) in MeCN-H_2O (1:1 v/v, PBS, pH 7.2).

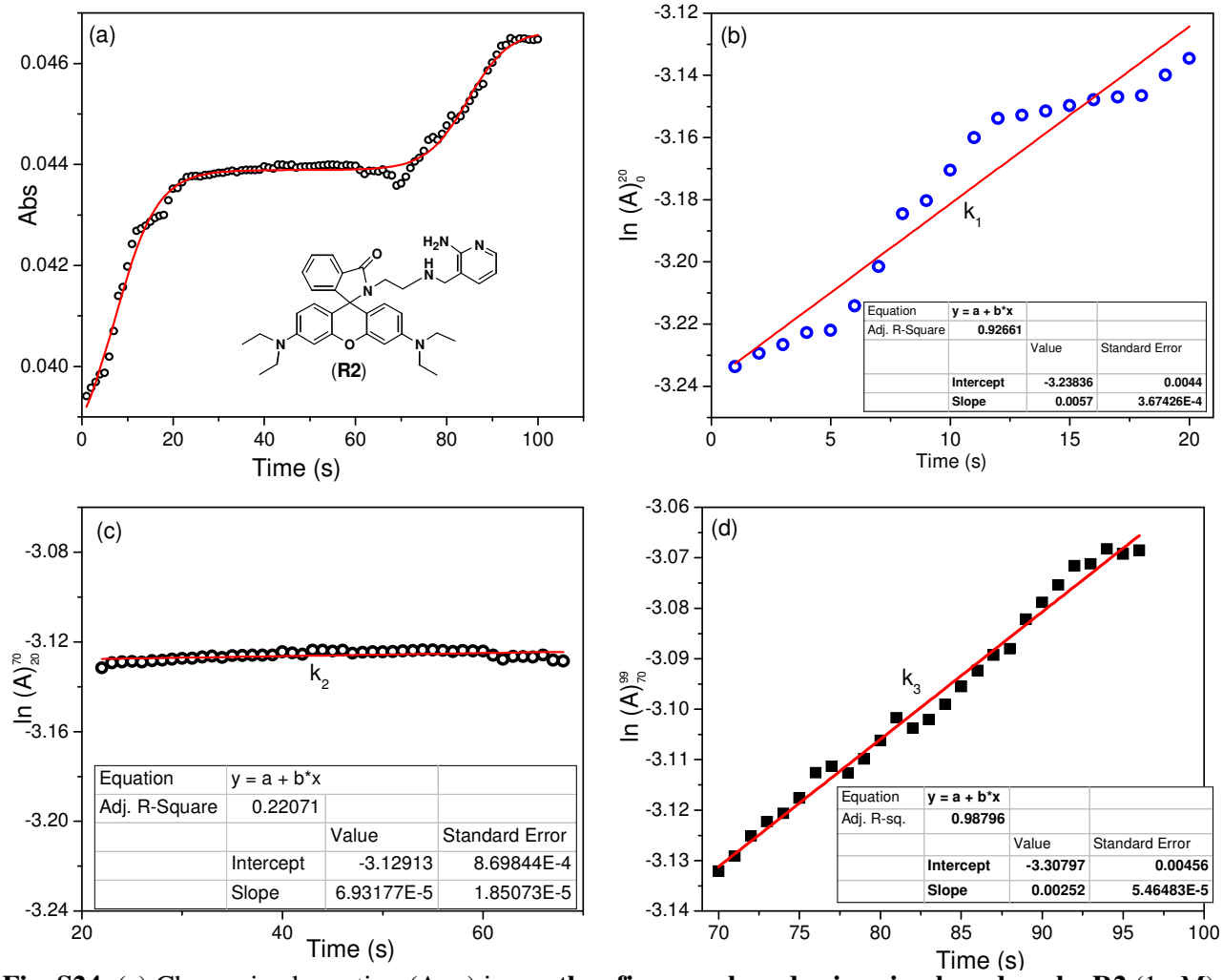

Fig. S24: (a) Change in absorption (A_{557}) in **another five membered spiro-ring based probe R2** (1 μM) when Hg^{2+} ion added in (1:2 ligand-metal stoichiometry) as a function of time (sec) in MeCN-H_2O (1:1 v/v, PBS, pH 7.2). Figures (b), (c) and (d) represents corresponding linear regression plots of ln(A_{557}) against time(s) for determination of fractional rate constants (k) of first-order kinetics at the desired time interval.

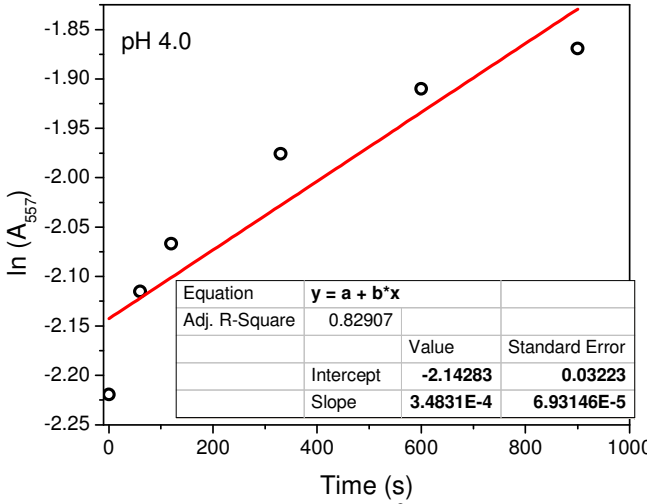

Fig. S25: Change in absorption (A_{557}) in **1**(10 μM) when Hg^{2+} ion (1:1 stoichiometry) added as a function of time (s) in MeCN-H_2O (1:1 v/v, PBS) at pH = 4.0.

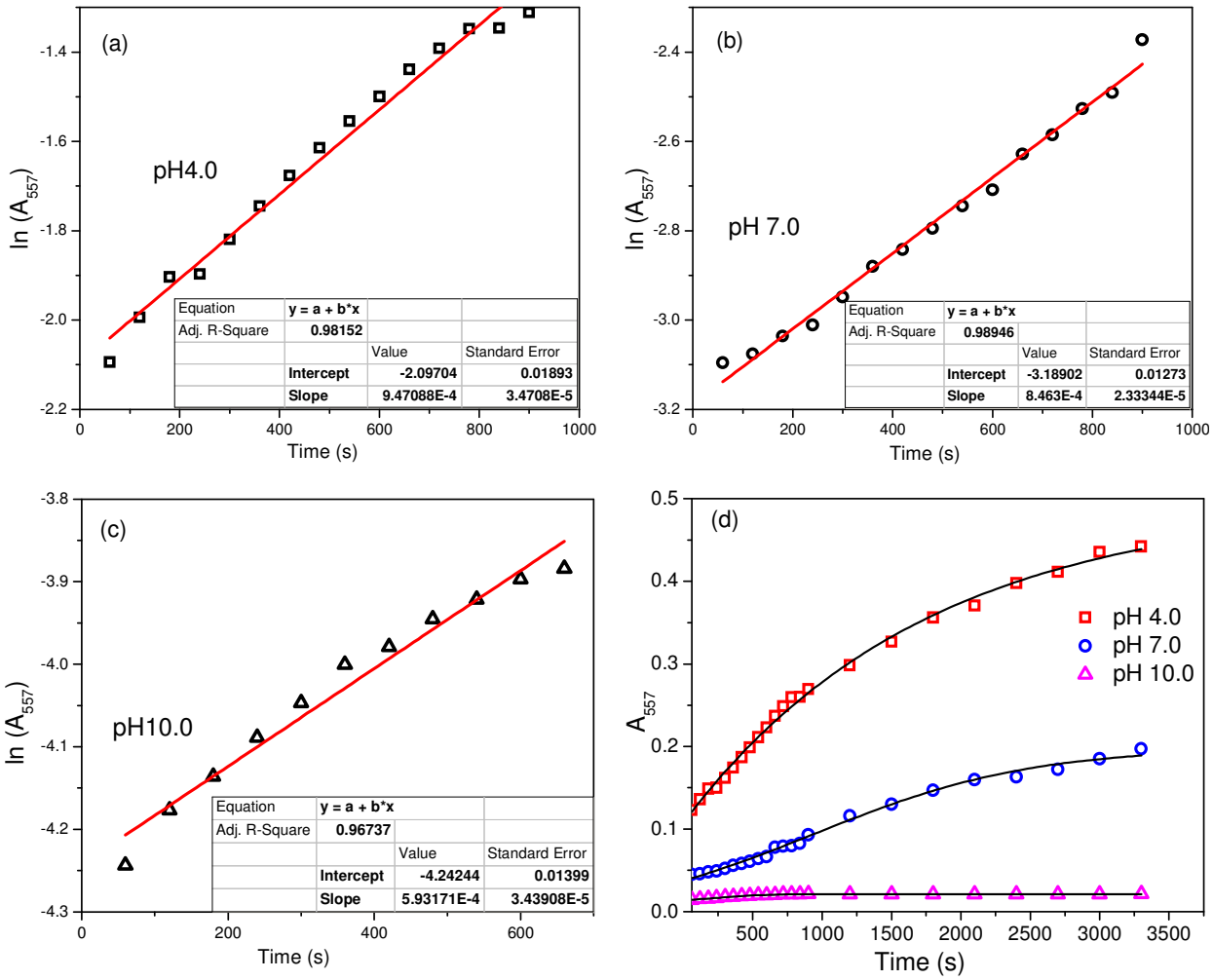

Fig. S26: Determination of rate of first order kinetics between **2** (10 μM) and Hg^{2+} (1 eq.) in at (a) 4.0, (b) 7.0 and (c) 10.0 pH from linear regression of the plot of log(A-A_0) as a function of time (s). $\lambda_{obs}^{(abs)}$ = 557nm. (d) Spectral profile of absorbance versus time (as given in Fig. 5b) for immediate reference.

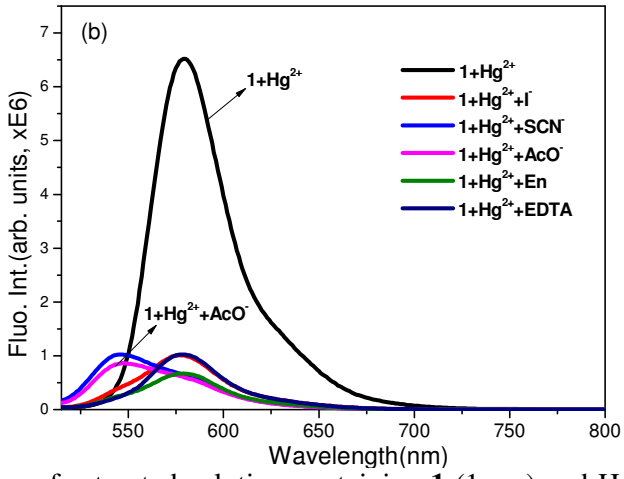

Fig. S27: Fluorescence spectra of saturated solution containing **1** (1 eq.) and Hg^{2+} (5 eq.) upon addition of anions and complexing reagents such as, SCN^-, EDTA, En, I^-, acetate ion (12eq.) in MeCN-H_2O (1:1v/v); [**1**] = 1μM, λ_{ex} = 500nm, RT, ex. and em. b p = 5nm.

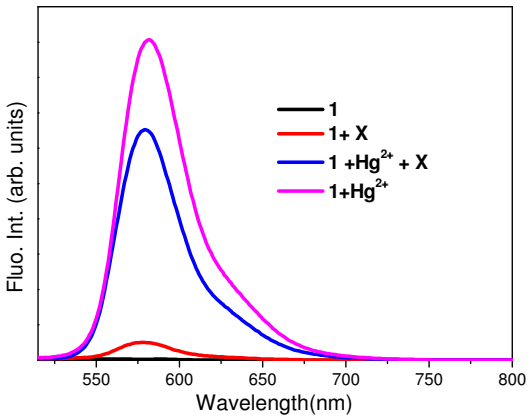

Fig. S28: Symbolic fluorescence spectra of **1** (1μM) with mixed metal ions (**X** = Pb^{2+}, Zn^{2+}, Cu^{2+}, Ni^{2+}, Fe^{2+}, Cd^{2+}, Co^{2+}, Mn^{2+}, and Ag^{+}, 10 μM, respectively) and upon addition of 1 eq. of Hg^{2+} ion, λ_{ex} = 500 nm.

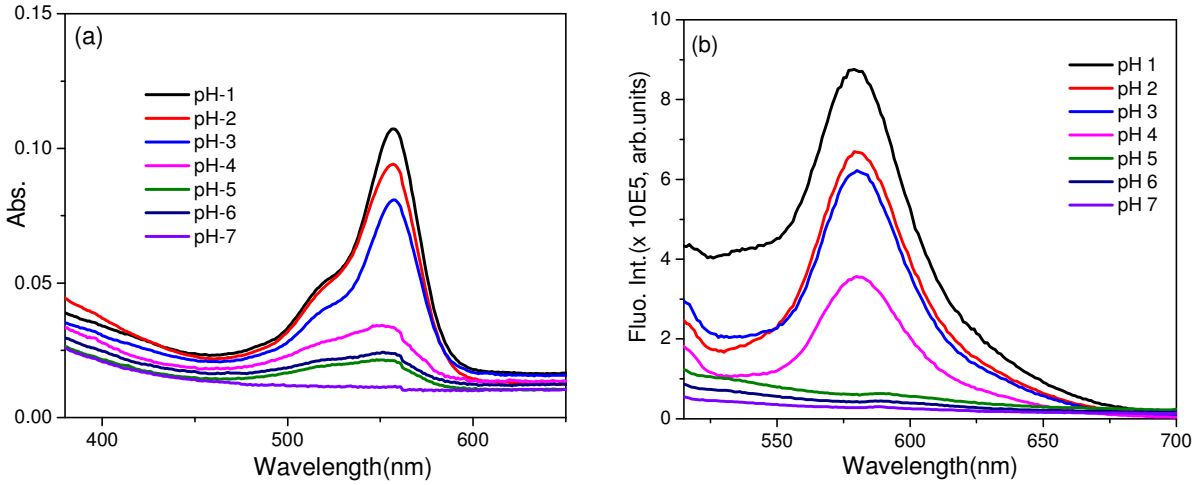

Fig. S29: Variation in (a) absorption (b) fluorescence intensity of **1** (10 μM) in MeCN-H_2O (1:9 v/v, PBS buffer) under different pH conditions.

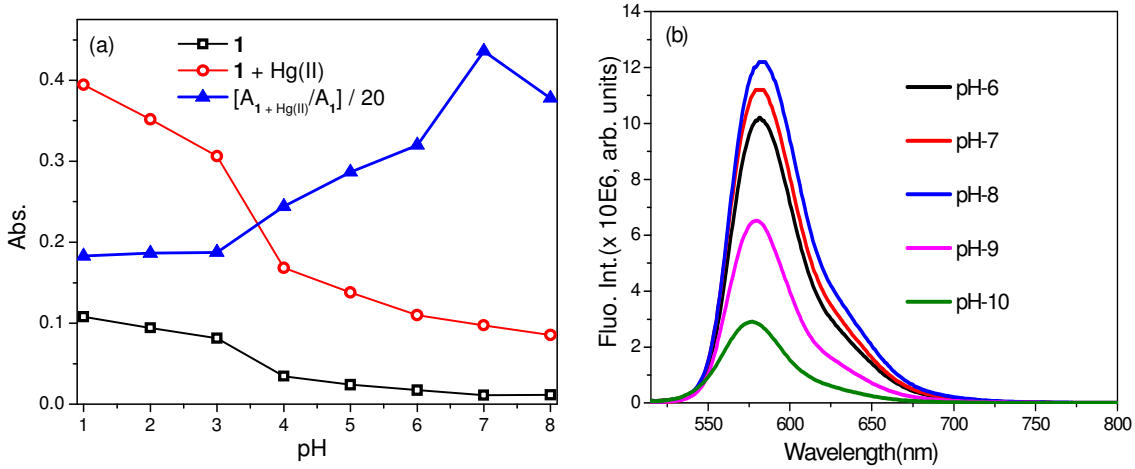

Fig. S30: (a) Change in absorption(A_{557}) of **1** (10 μM) in the presence of Hg^{2+} ion(1 eq.) in MeCN-H_2O (1:9 v/v, PBS buffer) under different pH conditions. Variation of fluorescence intensity (I_{580}) of **1** (1 μM) in presence of Hg^{2+} ion (5 eq.) in MeCN-H_2O (1:1 v/v, PBS buffer) at different pH, λ_{ex} = 500nm.

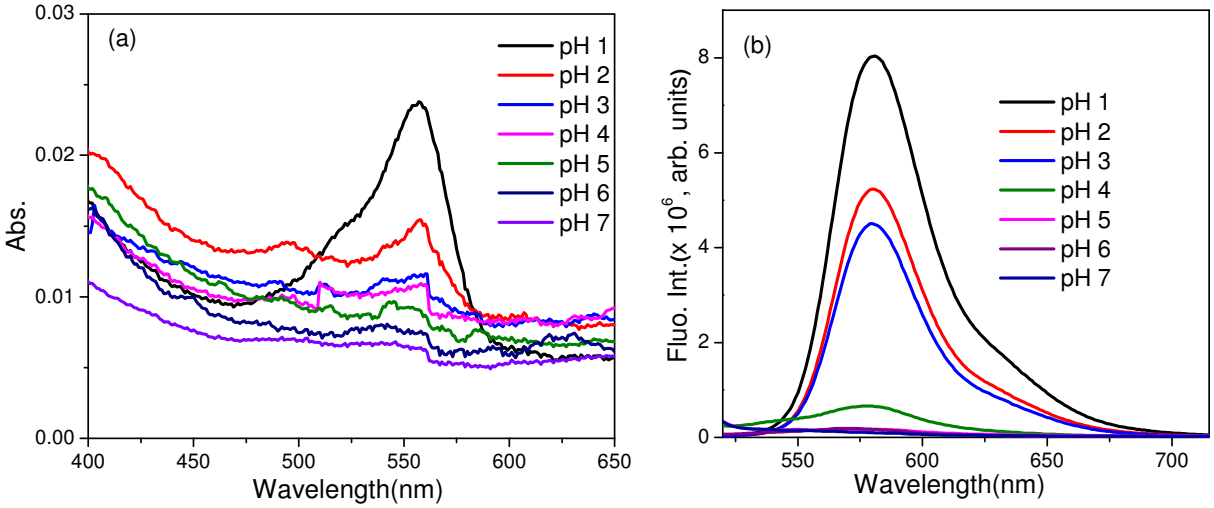

Fig. S31: Variation in (a) absorption (b) fluorescence intensity of **2** (10 μM) in MeCN-H_2O (1:9 v/v, PBS buffer) under different pH conditions.

Fig. S32: Colorimetric mapping of (a) **1** alone, (b) **1**+Hg^{2+} and (c) **2**+Hg^{2+} in MeCN-H_2O (1:9 v/v, PBS buffer) under different pH (pH = 1-8) conditions. [**1** or **2**] = 10 μM.

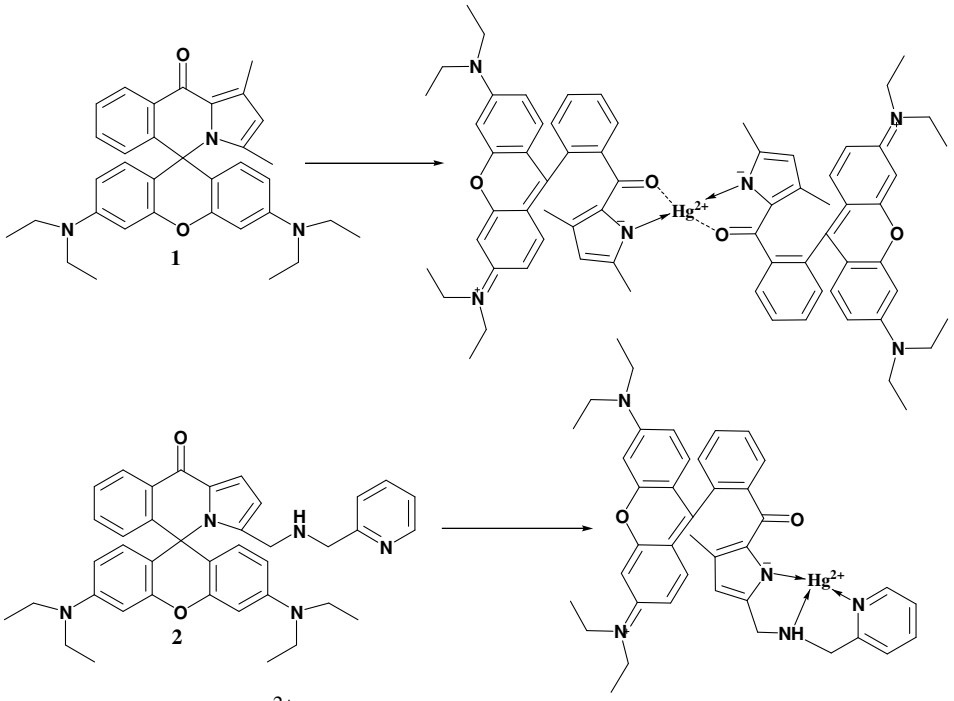

Fig. S33: Proposed mechanism of Hg^{2+} coordination to **1** and **2**.

*Bio-imaging with **1** for Hg^{2+} detection in E. Coli*

The biomass not treated with Hg^{2+} shows no fluorescence whereas treated biomass produced high fluorescence of rhodamine implying the significance of quantification of Hg^{2+} in biological system. The figure depicted below shows that Hg^{2+} could be possibly detected with even a low resolution fluorescence microscope.

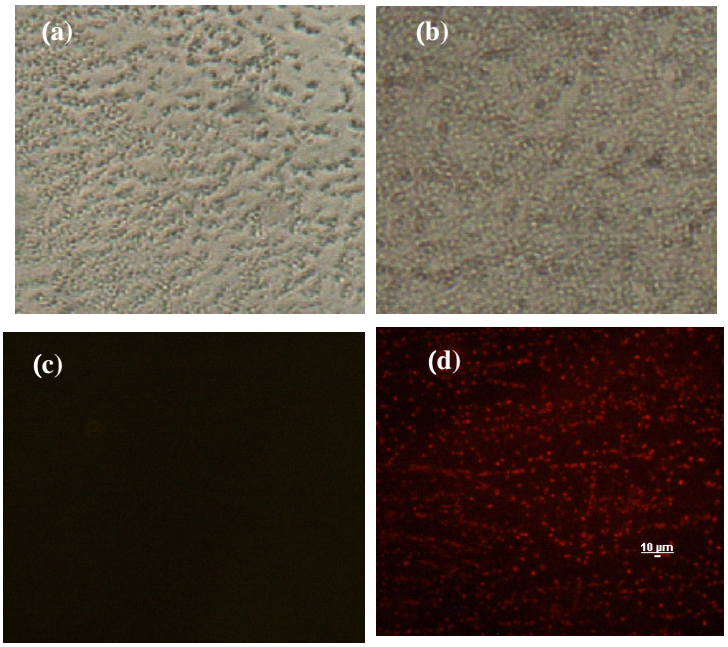

Fig. S34: Bright-field images of *E. Coli* alone (a) and after incubation with **1**(b). Their fluorescence image are on incubation with **1** before (c) and after (d) addition of Hg^{2+} ion, $\lambda_{ex} \approx 500$nm.